ELSEVIER

Journal of Molecular Structure (Theochem) 332 (1995) 105–126

THEO CHEM

An electronic and vibrational study of the cyclopropenyl ion and its fluoroderivatives

Sérgio E. Galembeck[a,1], Rui Fausto[b,*]

[a]*Departamento de Química Fundamental, Universidade Federal de Pernambuco, Av. Luis Freire s/n, Recife - PE, Brazil*
[b]*Departamento de Química, Universidade de Coimbra, P-3049 Coimbra, Portugal*

Received 16 May 1994; accepted 6 June 1994

Abstract

This article presents the results of ab initio SCF-MO calculations on both the electronic structure and vibrational spectra of the cyclopropenyl cation ($C_3H_3^+$) and its fluoroderivatives, $C_3H_2F^+$, $C_3HF_2^+$ and $C_3F_3^+$. A very simple and unambiguous criterion for choosing the combination of diffuse and polarization functions which, together with the 6-311G basis set, best describes the electron distribution in these ions is presented. The electronic structures of the cations are analysed in detail; particular emphasis is given to the analysis of the electronic effects due to successive hydrogen-by-fluorine replacements. The results of vibrational normal mode analysis carried out for all hydrogen–deuterium isotopomers of the studied ions are presented and compared with the available experimental data. The theoretical results are used both to review some band assignments previously proposed for the fluorosubstituted molecules and to give a stronger theoretical foundation to the general interpretation of the vibrational spectra of these compounds.

1. Introduction

The $C_3H_3^+$ ion has received considerable attention in recent years due to its high abundance in oxidative flames [1], and because it has been suggested as a possible soot precursor [2–4]. Recently this ion was detected in the coma of comet Halley, its probable origin being the dust particles around the comet [5]. Experimentally, two isomeric structures of $C_3H_3^+$ were observed: the cyclopropenyl (**CP**) and the propargyl cations [6,7] (Fig. 1), the first corresponding to the most stable isomer ($\Delta E = 109\,kJ\,mol^{-1}$ [6]). Theoretically, **CP** was also found to be the global energy minimum [8–12].

Because it is the simplest aromatic system, with two π electrons, **CP** presents great theoretical interest. In addition, it also exhibits σ-aromaticity, a property which is characteristic of three-membered cyclic systems. Indeed, both these factors contribute to stabilize this highly strained compound.

In the mid-fifties several derivatives of **CP** were prepared. However, only twenty years later were salts of the non-substituted ion isolated [13]. The large ^{13}C–H coupling constants observed for these systems suggested that the C–H bonds in **CP** should involve a carbon sp hybrid orbital. Thus, it was proposed that each carbon atom uses an sp

* Corresponding author.
[1] Permanent address: Departamento de Quimica, Faculdade de Filosofia, Ciências e Letras de Ribeirão Preto, Universidade de São Paulo, Av. dos Bandeirantes, 3900, 14040-901 Riberão Preto - SP, Brazil.

SSDI 0166-1280(94)03906-2

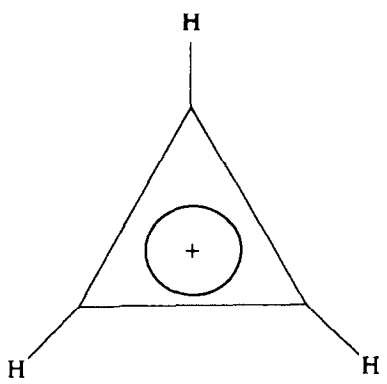

CP

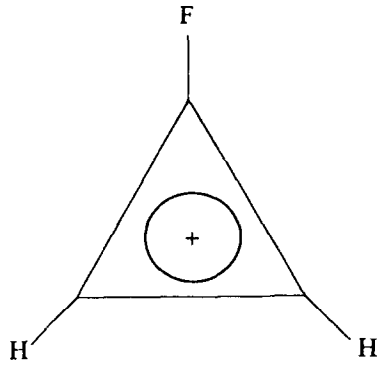

MFCP

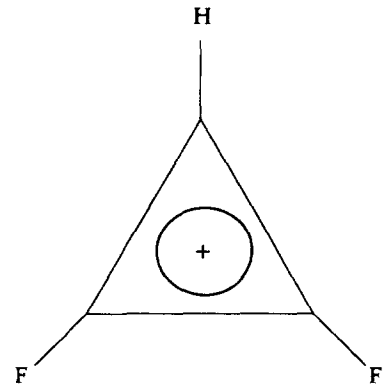

DFCP

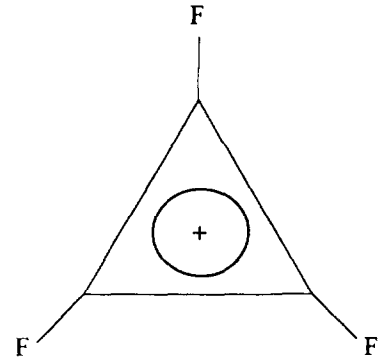

TFCP

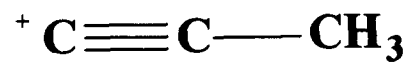

P

Fig. 1. Cyclopropenyl (**CP**), monofluorocyclopropenyl (**MFCP**), difluorocyclopropenyl (**DFCP**), trifluorocyclopropenyl (**TFCP**) and propargyl (**P**) cations.

orbital to form the C–H bond and two sp^3 hybrids in the ring plane to form the bent C–C σ bonds, while the remaining p orbital participates in the cation π system [13]. These conclusions were further supported by theoretical studies [14]. More recently, all the hydrogen–deuterium isotopomers of **CP** were prepared and studied by vibrational spectroscopy in both gaseous and condensed phases [15]. The experimental data indicated that both the f_{CC} and f_{CH} force constants are larger than those found in benzene, thus pointing to a stronger π bond in **CP** than in benzene.

Several theoretical studies, using different levels of approximation, have also been carried out on

CP. These include Hartree–Fock SCF calculations (using a minimal basis set [9], gaussian lobe functions [16] or double or triple-ζ plus polarization functions [8,10,12,17]), Møller–Plesset perturbation theory up to fourth order [11,18–20], interaction of configurations [14,19], and approximated coupled cluster methods [18,19]. In consonance with the experimental data, all these theoretical methods predict **CP** as a planar D_{3h} symmetric cation. In addition, the highest level theoretical calculations yield R_e(C–C) = 136.2–137.1 pm and R_e(C–H) = 107.5–108.3 pm [11,18–20]. However, it has been suggested [19] that the C–C bond lengths are probably overestimated by the theoretical calculations, whereas the C–H distances are slightly underestimated.

Two theoretical studies of the vibrational spectra of **CP** and its deuterated isotopomers were also reported [18,19]. These studies considered mainly the effects of the anharmonicity on the vibrational spectra of the molecule, and include the computation of both the harmonic and anharmonic force fields of **CP**, using post-Hartree–Fock methods. While these sophisticated calculations yielded results which agree very well with the experimental data, their generalization to more complex systems is as yet prohibitive in terms of computational facilities.

Despite the large number of theoretical studies on **CP** already published, none has looked at the electronic structure of this ion in great detail.

The three fluorosubstituted derivatives of **CP** (mono-, di- and trifluorocyclopropenyl cations — abbreviated, **MFCP**, **DFCP** and **TFCP**), including several deuterated species, have been prepared and studied by both Raman (in SO_2 solution) and infrared spectroscopy (in matrices) [21–23]. The vibrational data conform to a pattern of strengthening of C–C bonds due to fluorine substitution on a contiguous carbon atom and of weakening of the distal bond. In the trifluorosubstituted ion these effects were shown to cancel out [23]. In addition, both **MFCP** and **DFCP** were shown to have C_{2v} symmetry, while **TFCP**, like **CP**, belongs to the D_{3h} point group.

The fluorosubstituted cyclopropenyl ions have been little studied theoretically. In fact, to the best of our knowledge, only two papers on this subject were published. In the first [12], the equilibrium geometry and charge density distribution (Mulliken population analysis) of **MFCP** were calculated using a 6-31G* basis set. By comparing the results obtained for **MFCP** with those found for other monosubstituted cyclopropenyl ions, it was pointed out that fluorine appears to be the unique substituent that leads to the vicinal C–C bonds being longer than the distal one. In addition, it was proposed that the σ-withdrawing ability of the fluorine substituent should be more important than its π-donation ability. The second study [24] looked at **TFCP** at the SCF 3-21G and 6-31G* levels of calculation. Optimized geometries using both basis sets and the 3-21G Mulliken population analysis were reported, and the observed increase in the C–C bond lengths, when compared to those of **CP**, was also tentatively interpreted in terms of the σ-withdrawing and π-donation effects of the fluorine substituents. None of these calculations included diffuse functions within the basis set, despite the fact that it is well known that these are essential to adequately describe the electronic structure of strongly electronegative atoms [25].

In this paper we present the results of ab initio SCF-MO calculations on both the electronic structure and vibrational spectra of **CP** and its fluoroderivatives. In order to properly describe the electron distribution in these ions, the best combination of diffuse and polarization functions to be used, together with the 6-311G basis set, is first selected. To this end, in the first part of this paper, a very simple and unambiguous criterion for making the composition of the basis set (that may in principle be used successfully when substituents other than fluorine are considered) is presented. In the second part of this paper, the electronic structures of the cations are analysed in detail. Particular emphasis is given to the analysis of the electronic effects due to successive hydrogen-by-fluorine replacements. Finally, we present the results of vibrational calculations. Normal mode analysis are carried out for all hydrogen-deuterium isotopomers of the studied ions using the ab initio optimized geometries and force fields, and the results compared with the experimental data. The theoretical results are used both to review some band assignments previously proposed for the fluorosubstituted molecules and to give a stronger

theoretical foundation to the general interpretation of the vibrational spectra of these compounds.

2. Methods

Hartree–Fock SCF-MO calculations were carried out on a VAX (model 8820 or 6620) computer using the GAUSSIAN 90 system of programs [26]. Fully optimized geometries, constrained to the molecular point group, were determined for the studied molecules using the 6-311G basis set [27] without or with the systematic addition of polarization and/or diffuse functions [25] in "heavy atoms" (C, F) and H, covering all possible combinations (nine basis sets for **CP**, **MFCP** and **DFCP**, and four basis sets for **TFCP**). Vibrational frequencies were calculated analytically for all these basis sets to test the rank of the critical points, confirming that all optimized geometries correspond to minima in the potential energy hypersurface. Both the equilibrium geometries and vibrational frequencies were calculated using the default procedures of the program [26].

The force constants (symmetry internal coordinates) to be used in the normal coordinate analysis were obtained from the ab initio cartesian harmonic force constants using the program TRANSFORMER [28]. This program was also used to prepare the input data for the normal coordinate analysis programs used in this study (BUILD-G and VIBRAT [29]). The calculated force fields were scaled down by using a simple linear regression in order to adjust the calculated frequencies of the nine molecules studied (four isotopomers of **CP**, two of **MFCP** and **DFCP**, and one of **TFCP**) to the observed frequencies. Frequencies corresponding to unobserved or doubtfully assigned vibrations were then calculated from the ab initio force fields by interpolation using the straight line obtained previously. While very simple, this scaling procedure has the advantage, over the more elaborate force field scaling procedures which use several scale factors, of preserving the potential energy distributions (PEDs) as they emerge from the ab initio calculations. In addition, this method can also be used as a simple additional test of the quality of the electron distribution obtained with the basis set used to perform the MO calculations.

3. Results and discussion

3.1. Influence of the polarization and diffuse functions on the calculated electronic structures

Table 1 presents the calculated bond distances for **CP**. The largest changes in the calculated values due to the inclusion of polarization/diffuse functions in the basis set occur when the first polarization function (on the carbon atoms) is added: the C–C bond lengths become shorter, while the C–H bond lengths increase. The inclusion of both the second polarization (on the H atoms) and/or diffuse functions does not affect significantly the calculated geometry. It is interesting to note that this result agrees with previous studies, suggesting that the most important factors that affect the bond lengths calculated with a given basis set are (i) the presence (or absence) of polarization functions in non-hydrogen atoms and (ii) electron correlation [11,18,19]. Indeed, the bond lengths now obtained are shorter than those previously determined using methods that include electron correlation (C–C: 136.2–137.1 pm; C–H: 107.5–108.3 pm [11,18–20]). Table 1 also shows that the inclusion of polarization functions on the carbon atoms leads to shorter C···H non-bonded distances, while the H···H non-bonded distances remain

Table 1
Basis set dependence of the calculated bond lengths and distances between non-bonded atoms (pm) of **CP**

Basis[a]	C–H	C–C	C···H	H···H
G	106.4	136.2	234.4	320.5
+G	106.5	136.2	234.5	320.6
++G	106.5	136.2	234.5	320.6
G*	107.1	135.0	234.0	320.5
+G*	107.1	135.0	234.0	320.5
++G*	107.1	135.0	234.0	320.6
G**	107.2	135.0	234.0	320.6
+G**	107.2	134.9	234.0	320.6
++G**	107.1	135.0	234.0	320.6

[a] Abbreviated. +G* represents the 6-311+G* basis set.

Table 2
Basis set dependence of the calculated bond lengths (pm) of **MFCP**, **DFCP** and **TFCP**

Basis[a]	**MFCP**				**DFCP**				**TFCP**	
	C–F	C–H	C(F)–C(H)	C(H)–C(H)	C–F	C–H	C(F)–C(H)	C(F)–C(F)	C–F	C–C
G	128.8	106.5	135.0	137.5	128.4	106.7	136.2	134.5	128.1	135.6
+G	128.6	106.6	135.0	137.5	128.2	106.7	136.3	134.6	127.8	135.8
++G	128.6	106.6	135.1	137.5	128.2	106.7	136.3	134.6		
G*	124.1	107.2	134.4	136.3	123.9	107.3	135.6	134.4	123.7	135.6
+G*	124.1	107.2	134.3	136.3	123.8	107.3	135.6	134.4	123.6	135.6
++G*	124.1	107.3	134.3	136.3	123.8	107.3	135.6	134.4		
G**	124.1	107.3	134.3	136.3	123.9	107.5	135.6	134.3		
+G**	124.1	107.3	134.3	136.3	123.8	107.4	135.6	134.4		
++G**	124.1	107.3	134.3	136.3	123.8	107.4	135.6	134.4		

[a] Abbreviated. +G* represents the 6311+G* basis set.

constant upon inclusion of either diffuse or polarization functions.

Table 2 shows the calculated bond distances for the fluorosubstituted cyclopropenyl ions. The general pattern of variation with the basis set is similar to that observed for **CP**. The inclusion of polarization functions makes the "heavy atom–heavy atom" (C–F and C–C) bond lengths shorter and the C–H bond lengths longer. The inclusion of diffuse functions gives rise to very small (less than 0.3 pm) and non-systematic changes in bond lengths.

For symmetry reasons, the bond angles of both **CP** and **TFCP** do not depend on the basis set. In turn, the calculated changes in the bond angles of **MFCP** and **DFCP** due to the addition of polarization or diffuse functions to the basis set do not exceed 1°.

Table 3 shows the dependence on the basis set of both the total energies and heats of formation calculated with or without including zero-point energy corrections. From these data, it can be concluded that the basis set dependence of the calculated energies conform to a pattern similar to that followed by their geometries (Tables 1 and 2). In particular, the inclusion of the first polarization function produces the largest changes. Hence, both energetic and geometric results clearly indicate that the addition of polarization functions on the non-hydrogen atoms to the 6-311G basis set is required to improve the performance. However, in order to evaluate the general quality of a given basis set, a systematic analysis of the electron distribution it yields is crucial.

Table 4 presents the gross (χ_g) and the net (χ_n) Mulliken atomic electron populations for **CP** calculated with the various basis sets used. The gross charges on the carbon atoms ($q(c) = 6 - \chi_g$) are near zero for the 6-311G basis set. The addition of a diffuse function on these atoms increases their gross electron population. A further increase is observed upon the addition of the second diffuse function (on the hydrogen atoms). On the contrary, the addition of the first polarization function (on the carbon atoms) to the basis set produces only a very small increase in the carbon gross electron population, whereas the addition of the second one (on the hydrogen atoms) makes the gross charge of the carbon atoms slightly positive. The net charges on the carbon atoms present a quite different pattern. Thus, the addition of polarization functions (either on the carbon or on the hydrogen atoms) leads to an electron charge transfer from the carbon atoms to both the overlap terms (χ_0(C–C) and χ_0(C–H)) and hydrogen atoms; the addition of the first diffuse function produces a decrease in the net electron population of the carbon atoms, whereas the addition of the second one increases the net electron population of these atoms to a higher value than the initial one.

Table 4 also presents the total C–C and C–H overlap populations. It is important to note that several basis sets represent the C–C bonds as having a smaller (or nearly equal) overlap population than the C–H bonds. Obviously, this result is not reasonable, since the C–C bonds are known to

Table 3
Basis set dependence of the calculated total energies (E), heats of formation (ΔH_f), zero point energies (ZPE) and heats of formation corrected to zero point energies (ΔH_f^{corr}) of **CP**, **MFCP**, **DFCP**, **TFCP**[a]

Basis[b]	**CP**				**MFCP**				**DFCP**				**TFCP**			
	E	ΔH_f	ZPE	ΔH_f^{corr}	E	ΔH_f	ZPE	ΔH_f^{corr}	E	ΔH_f	ZPE	ΔH_f^{corr}	E	ΔH_f	ZPE	ΔH_f^{corr}
G	−114.95928	192.0	125.9	191.6	−213.78013	289.9	107.1	288.7	−312.59770	392.5	87.4	389.5	−411.41196	498.3	16.2	494.1
+G	−114.95993	190.4	125.9	190.0	−213.78279	283.2	106.3	280.7	−312.60259	379.5	86.2	375.3	−411.41940	478.6	15.7	472.4
++G	−114.96004	190.4	125.9	189.5	−213.78290	282.8	106.3	280.7	−312.60268	379.1	86.2	375.3				
G*	−115.02412	21.7	126.8	22.2	−213.88294	20.1	108.8	20.5	−312.73999	18.8	90.4	18.8	−411.59496	18.0	17.2	18.0
+G*	−115.02502	19.2	126.4	19.7	−213.88570	13.0	108.8	13.0	−312.74470	6.3	90.4	6.7	−411.60177	0.0	17.2	0.0
++G*	−115.02507	19.2	126.8	19.7	−213.88573	13.0	108.8	13.0	−312.74471	6.3	90.4	6.7				
G**	−115.03161	2.1	126.4	2.1	−213.88294	20.1	108.8	20.5	−312.74242	12.6	90.4	12.6				
+G**	−115.03234	0.1	126.4	0.1	−213.89055	0.1	108.4	0.1	−312.74711	0.4	90.4	0.4				
++G**	−115.03239	0.0	126.4	0.0	−213.89059	0.0	108.4	0.0	−312.74714	0.0	90.4	0.0				

[a] Total energies in hartrees (1 hartree = 2625.5001 kJ mol^{-1}); all other quantities in kJ mol^{-1}. The heats of formation presented in this table correspond to relative values, taking those obtained with the 6-311++G** basis set as reference values.
[b] Abbreviated: +G* represents the 6-311+G* basis set.

Table 4
Basis set dependence of the calculated gross (χ_g) and net (χ_n) Mulliken atomic populations and overlap (χ_O) populations of **CP**[a]

Basis[b]	χ_g(C)	σ_g(C)	π_g(C)	χ_g(H)	χ_n(C)	σ_n(C)	π_n(C)	χ_n(H)	χ_O(C–C)	σ_O(C–C)	π_O(C–C)	χ_O(C–H)
G	6.008	5.341	0.667	0.659	5.433	5.110	0.323	0.315	0.116	−0.004	0.120	0.353
+G	6.047	5.380	0.667	0.620	5.079	4.755	0.324	0.291	0.320	0.201	0.120	0.346
++G	6.119	5.452	0.667	0.548	5.595	5.271	0.324	0.293	0.132	0.013	0.120	0.383
G*	6.014	5.347	0.667	0.653	5.052	4.752	0.301	0.308	0.308	0.177	0.132	0.366
+G*	6.032	5.389	0.643	0.634	4.783	4.481	0.301	0.293	0.454	0.323	0.132	0.310
++G*	6.074	5.407	0.667	0.593	5.289	4.988	0.301	0.280	0.237	0.105	0.132	0.332
G**	5.889	5.225	0.664	0.778	4.992	4.695	0.297	0.392	0.255	0.124	0.132	0.415
+G**	5.913	5.249	0.664	0.754	4.633	4.485	0.298	0.369	0.447	0.316	0.131	0.369
++G**	5.967	5.303	0.664	0.700	4.888	4.590	0.298	0.336	0.358	0.227	0.131	0.348

[a] In units of e ($e = 1.60219 \times 10^{-19}$ C); π_g(H), π_n(H) and π_O(C–H) are not presented as they have been found to be negligible.
[b] Abbreviated. +G* represents the 6-311+G* basis set.

have a considerable double bond character. From this point of view, only the 6-311+G* and 6-311+G** basis sets can be considered to yield proper results, pointing to the relevance of the presence of a diffuse function on the carbon atoms, in addition to the polarization function.

From the analysis of the π and σ gross, net and overlap populations calculated for **CP** (Table 4), it can be concluded that:

(i) The π gross and net electron populations do not change very much with the addition of either diffuse or polarization functions. This result indicates that both polarization and diffuse functions are more important to the description of the σ system than to the description of the π system. In fact, the changes in the total atomic populations with the addition of these functions to the basis set are essentially equal to those observed in the σ populations.

(ii) The σ/π partition of the C–C overlap populations yields very interesting results. For instance, the 6-311G basis set fails to account for a C–C σ bond. In addition, several other basis sets herein studied yield a C–C π overlap population, π_O(C–C), greater than or equal to the σ one, σ_O(C–C). Indeed, only two basis sets among the whole set considered (6-311+G* and 6-311+G**) do not fail to predict properly the ratio π_O(C–C)/σ_O(C–C) which, considering the π-bond order of a C–C symmetrically delocalized partial double bond in a three-membered cyclic molecule, must be close to 0.33.

Table 5 presents both C–C and C–F σ and π overlap populations for **DFCP**. It can be concluded from this table and from similar data

Table 5
Basis set dependence of the calculated overlap populatins between "heavy atoms" of **DFCP**[a]

Basis[b]	π_O(C–F)	σ_O(C–F)	π_O(C(H)–C(F))	σ_O(C(H)–C(F))	π_O(C(F)–C(F))	σ_O(C(F)–C(F))
G	0.028	0.207	0.119	−0.258	0.107	−0.124
+G	0.028	0.212	0.119	−0.269	0.108	−0.239
++G	0.028	0.235	0.119	−0.714	0.109	0.128
G*	0.067	0.277	0.136	−0.017	0.120	0.138
+G*	0.059	0.133	0.138	0.255	0.130	0.177
++G*	0.059	0.146	0.138	0.128	0.125	0.265
G**	0.067	0.276	0.135	−0.021	0.113	0.131
+G**	0.058	0.127	0.137	0.222	0.129	0.128
++G**	0.058	0.139	0.137	0.140	0.130	0.210

[a] In units of e ($e = 1.60219 \times 10^{-19}$ C).
[b] Abbreviated. +G* represents the 6-311+G* basis set.

obtained for **MFCP** and **TFCP** (not shown here in the interest of brevity; complete results are available from the authors) that the inclusion of polarization functions on non-hydrogen atoms (carbon, fluorine) produces large changes in the calculated π overlap populations, whereas the presence of polarization functions on hydrogen atoms does not significantly affect these populations. In turn, the addition of diffuse functions to the 6-311G basis set without polarization functions does not affect π overlap populations, whereas the inclusion of diffuse functions to the 6-311G* or 6-311G** basis produces small changes on both C–F and C(H)–C(F) π overlap populations. On the contrary, the C(F)–C(F) π overlap is much more sensitive to the addition of diffuse functions to the basis sets which also have polarization functions, though a systematic trend of variation cannot be established. The σ overlap populations are much more sensitive to the basis set than the π ones. Thus, the first polarization function (on carbon and fluorine atoms) gives rise to a general increase of the σ overlap populations, while the second (on hydrogen atoms) has a small effect in the opposite direction. In turn, the single addition of diffuse functions to the 6-311G basis set increases the C–F and decreases the C(H)–C(F) σ overlap populations, also affecting significantly the C(F)–C(F) σ overlap population, although in a non-systematic way. A non-systematic pattern of variation of σ populations also occurs when diffuse functions are successively added to those basis sets which have polarization functions.

It is particularly interesting that the results presented in Table 5 show that all basis sets predict that the C–F π overlap is smaller than C–F σ, which is in consonance with the well-known small π donation ability usually exhibited by the fluorine atoms. In addition, it can also be noted that when the basis set does not include at least one diffuse and one polarization function, the calculated C–C σ overlap populations present negative values. Thus, only four basis sets among the whole set of basis studied do not present this failure: 6-311+G*, 6-311++G*, 6-311+G** and 6-311++G**. However, both the 6-311++G* and 6-311++G** basis sets yield π_O(C(H)–C(F))/σ_O(C(H)–C(F)) ratios close to one, while 6-311+G** yields the π_O(C(F)–C(F))/σ_O(C(F)–C(F)) ratio equal to one, thus predicting C–C bonds with a double bond character too large for a conjugated system. Thus, also in the case of the fluorosubstituted cyclopropenyl ions, the population analysis results indicate that, among the whole set of basis studied, the 6-311+G* basis is that which yields the best representation of the electron distribution. In fact, the two above-mentioned ratios exhibit reasonable values when calculated using this basis set (π_O(C(H)–C(F))/σ_O(C(H)–C(F)) = 0.62; π_O(C(F)–C(F))σ_O(C(F)–C(F)) = 0.71).

In summary, Mulliken population analysis results provide evidence that both polarization and diffuse functions on carbon and fluorine atoms must be added to the 6-311G basis set in order to reach an adequate description of the electronic density of the molecules studied. In turn, the additional presence of diffuse or polarization functions on hydrogen atoms does not improve the results, and may even make them worse. Indeed, it must be stressed that these results further reinforce the conclusions of previous studies undertaken on different molecules [25,30,31] which pointed out the necessity of including diffuse functions to adequately describe the electron density of molecules having strongly electronegative atoms, in particular when the 6-311G basis set is used.

It has been pointed out frequently that Mulliken charges are quite sensitive to changes in the basis set and usually do not converge to a given value upon increasing the basis set size [32]. On the contrary, the charges obtained using the charge–charge flux–overlap (CCFO) model [33] present very good stability with respect to changes in the basis set, since in general this model is able to represent properly the electron distribution of a given molecule [34]. Thus, we have decided to test the reliability of the method presented above to choose the best basis set by also looking at the basis set dependence of the charges obtained from the CCFO model.

In Table 6 the CCFO derived atomic charges (q^C) for **CP** are compared with those obtained from the Mulliken partition analysis (q^M; see also Table 4). From this table it can be concluded that for this molecule the addition of a polarization function to the 6-311G basis set increases the positive charge of the carbon atoms and reduces that of the hydrogens, while the addition of the second set of polarization

Table 6
Basis set dependence of the atomic charges of **CP** calculated using the Mulliken atomic partition criterion (q^M) and the CCFO model (q^c)[a]

Basis[b]	q^c(C)	q^M(C)	q^c(H)	q^M(H)
G	0.098	−0.008	0.235	0.341
+G	0.095	−0.047	0.238	0.380
++G	0.098	−0.119	0.235	0.452
G*	0.148	−0.014	0.185	0.347
+G*	0.148	−0.032	0.185	0.366
++G*	0.149	−0.074	0.185	0.407
G**	0.146	0.111	0.188	0.222
+G**	0.147	0.087	0.185	0.245
++G**	0.146	0.033	0.187	0.300

[a] In units of e ($e = 1.60219 \times 10^{-19}$ C).
[b] Abbreviated. +G* represents the 6-311+G* basis set.

functions or diffuse functions does not produce any significant change in the CCFO charges.

It is interesting to note that the Mulliken charges do not exhibit a similar behavior, but both the calculated net atomic populations on the carbon atoms and the C–C overlap populations (see Table 4) are consistent with the CCFO derived atomic charges. In particular, as was already referred to, the results obtained for these two properties indicate that the addition of the first set of polarization functions leads to an electron density transfer from the carbon atoms to both the C–C overlap and hydrogens. Thus, the changes observed in the CCFO charges may be correlated with those observed for C–C bond lengths (a decrease in this bond length is observed upon inclusion of the first set of polarization functions — see Table 1).

Table 7
Basis set dependence of the atomic charges of **MFCP**, **DFCP** and **TFCP** calculated using the Mulliken atomic partition criterion (q^M) and the CCFO model (q^c)[a]

Basis[b]	q^c(C(H))	q^M(C(H))	q^c(C(F))	q^M(C(F))	q^c(H)	q^M(H)	q^c(F)	q^M(F)
MFCP								
G	0.060	0.047	0.480	0.403	0.257	0.359	−0.114	−0.215
+G	0.075	0.183	0.447	0.115	0.252	0.400	−0.103	−0.283
++G	0.079	0.248	0.443	−0.267	0.202	0.482	−0.074	−0.192
G*	0.099	0.023	0.466	0.428	0.206	0.356	−0.077	−0.095
+G*	0.112	0.085	0.445	0.191	0.202	0.380	−0.077	−0.121
++G*	0.113	0.080	0.443	0.119	0.202	0.418	−0.074	−0.116
G**	0.100	0.106	0.463	0.420	0.206	0.230	−0.076	−0.091
+G**	0.116	0.172	0.437	0.269	0.202	0.254	−0.072	−0.122
++G**	0.117	0.186	0.435	0.127	0.202	0.309	−0.071	−0.116
DFCP								
G	0.017	0.105	0.444	0.460	0.283	0.376	−0.091	−0.200
+G	0.044	0.340	0.425	0.410	0.272	0.418	−0.083	−0.289
++G	0.048	0.474	0.424	0.281	0.270	0.518	−0.083	−0.277
G*	0.041	−0.018	0.419	0.411	0.231	0.365	−0.055	−0.085
+G*	0.069	0.184	0.407	0.340	0.223	0.390	−0.053	−0.127
++G*	0.071	0.314	0.406	0.252	0.223	0.429	−0.053	−0.123
G**	0.043	0.114	0.418	0.407	0.231	0.238	−0.055	−0.083
+G**	0.075	0.227	0.404	0.383	0.221	0.262	−0.052	−0.127
++G**	0.075	0.388	0.404	0.270	0.221	0.318	−0.052	−0.123
TFCP								
G			0.399	0.520			−0.066	−0.187
+G			0.393	0.619			−0.059	−0.286
G*			0.363	0.409			−0.030	−0.076
+G*			0.362	0.460			−0.029	−0.127

[a] In units of e ($e = 1.60219 \times 10^{-19}$ C).
[b] Abbreviated. +G* represents the 6-311+* basis set.

Table 7 presents the CCFO and Mulliken atomic charges for the fluorosubstituted cyclopropenyl ions. The additon of both diffuse and polarization functions generally increases q^c(C(H)) and q^c(F), and decreases q^c(C(F)) and q^c(H). However, after the addition of the first polarization and diffuse functions (i.e. for the 6-311+G* basis set) all q^c values have already practically converged. Thus, once again, the 6-311+G* basis set appears as the smallest basis set among those considered which is able to describe well the electronic structure of both **CP** and its fluoroderivatives.

It is also interesting to note that, as was found for the non-substituted ion, a correlation between the CCFO charges (not the Mulliken ones) and both the Mulliken overlap populations and bond lengths may also be established for the fluorine-containing compounds. Thus, fluorine atoms lost electronic density to the C–F overlap and C(F) atoms with the increase of the basis set, leading to a less negative charge on the fluorine atoms and to a less positive charge on the C(F) atoms. In turn, C(H) transfers electronic density to all overlaps and atoms bonded to this atom (i.e. the charge on C(H) becomes more positive and the charge on hydrogen less positive). Finally, a decrease in a given C–C or C–F bond length correlates with both an increase in the corresponding overlap population and a decrease of the CCFO charges (absolute values) of the atoms making the bond.

In summary, the analysis of the dependence on the basis set of bond lengths, energies, Mulliken atomic and overlap populations, and CCFO charges calculated for the non-substituted as well as for the various fluorosubstituted cyclopropenyl ions studied clearly indicates that the smallest basis set which yields reliable results for the four molecules considered is the 6-311+G*. The method used here to choose the basis set is very simple, and is mainly based on a property that is calculated by almost all program packages used to carry out ab initio MO calculations.

*3.2. Effects of fluorine substitution on the electronic structure of **CP***

Table 8 shows the 6-311+G* calculated C–C and C–F bond lengths for a series of organic com-

Table 8
C–C and C–F bond lengths (pm) of **CP**, **MFCP**, **DFCP**, **TFCP** and several related molecules calculated with the 6-311+G* basis set

Molecule	C(H)–C(H)	C(H)–C(F)	C(F)–C(F)	C–F
Ethane	152.7			
Fluoroethane		151.1		137.4
Ethylene	131.9			
Fluoroethylene		130.9		132.6
Acetylene	118.3			
Fluoroacetylene		117.4		126.0
Cyclopropane	150.1			
Fluorocyclopropane	151.6	148.2		125.4
Cyclopropene	149.9 (C–C)			
	127.6 (C=C)			
1-Fluorocyclopropene	154.3	146.0		129.3
		126.5		
3-Fluorocyclopropene	128.9	145.7		137.4
Allyl cation	137.3			
1-Fluoroallyl cation	136.1	138.5		125.7
2-Fluoroallyl cation		136.8		130.4
Cyclopropyl cation	144.0 (C_1–C_2)			
	151.4 (C_2–C_3)			
1-Fluorocyclopropyl cation	156.9	142.0		122.0
CP	135.0			
MFCP	136.3	134.3		124.1
DFCP		135.6	134.4	123.8
TFCP			123.6	123.6

pounds and some of their fluorine-substituted derivatives. From this table, the following conclusions can be drawn:

(i) As could be anticipated, the C–C bonds in **CP** have a considerable double bond character, the C–C bond length being in between those found for ethane and ethylene (or in between the single and double bonds of cyclopropene). In addition, the calculations indicate that the C–C bond length in **CP** has a greater double bond character (i.e. it is shorter) than in the allyl cation. These results agree with a previous experimental study [15], which has suggested that the C–C bonds in **CP** should be stronger than in benzene.

(ii) As found for other three-membered cyclic compounds [12,35–39], the H → F substitution leads to a shortening of the vicinal C–C bonds and to an increase of the bond length of the distal C–C bond. These results are in consonance with a relative decrease in the p character of the carbon sp^3 hybrid orbitals involved in the σ vicinal C–C bonds. This decrease of p character of the carbon sp^3 hybrid orbitals is accompanied by an increase in p character of the carbon sp hybrid orbital used to make the bond with the fluorine atom, a result which agrees with the expected net electron withdrawing ability of the fluorine substituent. Indeed, it is well known that, in general, the amount of p character of a carbon orbital involved in a bond increases with the withdrawing ability of the substituent [40]. Furthermore, this intepretation is reinforced by looking at the calculated relative values of the bond angles around a fluorosubstituted or an unsubstituted carbon atom in the studied ions (Fig. 2). For example, the C–C(F)–C angle is larger than the C–C(H)–C one because the C(F) atom uses hybrid orbitals with larger s character to make the C–C bonds than the C(H) atom. In addition, the F–C–C(F) and H–C–C(F) angles are larger than the F–C–C(H) and H–C–C(H) angles, respectively, because the central carbon atoms use an hybrid orbital with larger s character to make the C–C(F) bond than the C–C(H) bond.

(iii) The second H → F substitution leads to an increase in the C(F)–C(H) bond length, while the C(F)–C(F) bond length assumes a value nearly equal to that of the C(F)–C(H) bond in **MFCP**. The first observation correlates with a decrease in the s character of the sp^3 hybrids orbitals of the C(H) atom (this atom is now bonded to two C(F) atoms, which are more electronegative than a C(H) atom), while the second one indicates that the hybridization of the C(F) atom is not significantly affected by the presence of a second fluorine substituent (certainly because opposite effects due to the substitution cancel out to a large extent). This last result agrees with vibrational data [21,22] which have revealed that the force constants associated with the C(F)–C(H) bond in **MFCP** and with the C(F)–C(F) bond in **DFCP** do not differ significantly.

(iv) The calculated changes in bond lengths and angles due to the third H → F substitution can also be explained considering changes in the relative s/p

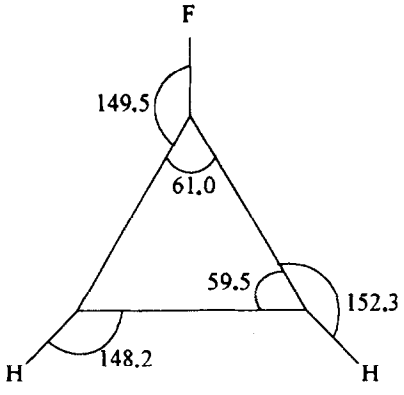

MFCP

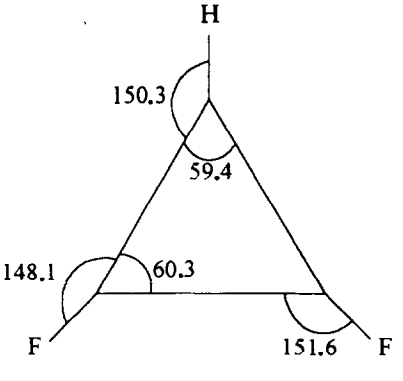

DFCP

Fig. 2. 6-311+G* calculated bond angles (degrees) of **MFCP** and **DFCP**.

Table 9
Mulliken gross populations of **CP**, **MFCP**, **DFCP** and **TFCP**, calculated with the 6-311+G* basis set[a]

Molecule	χ_g(C(H))	π_g(C(H))	σ_g(C(H))	χ_g(C(F))	π_g(C(F))	σ_g(C(F))	χ_g(F)	π_g(F)	σ_g(F)	χ_g(H)
CP	6.032	0.643	5.389							0.634
MFCP	5.915	0.683	5.232	5.809	0.794	5.014	9.121	1.841	7.280	0.620
DFCP	5.816	0.709	5.107	5.660	0.806	4.855	9.127	1.840	7.287	0.610
TFCP				5.540	0.827	4.713	9.127	1.840	7.287	

[a] In units of e ($e = 1.60219 \times 10^{-19}$ C).

contributions to the σ-system hybrid orbitals of the carbon atoms. In particular, the C–C bond length increases, due to the decreased s character of the hybrid orbitals of the carbon atoms used to make the C–C bonds.

(v) The C–F bond lengths decrease slightly with the number of fluorine atoms, showing that the s character of the carbon orbitals used to make the C–F bonds increases with the number of fluorine atoms, and thus being in agreement with the above conclusions taken mainly by analysis of the influence of the H → F substitutions on the C–C bond lengths.

(vi) Finally, by comparing the C–F bond lengths in the fluorosubstituted cyclopropenyl ions with those obtained for almost all the remaining compounds considered in Table 8, it can be concluded that in the studied cations this bond is very short. This may be due, at least in part, to an increased double bond character of this bond in the studied ions.

Table 9 presents the Mulliken gross atomic populations and their σ/π components for the studied ions. The total atomic populations of the carbon atoms, as well as their σ components, reduce with the number of fluorine atoms, showing that the fluorine atoms act as σ electron withdrawing substituents. As expected, the total atomic population of the C(H) atoms is always larger than that of the C(F) atoms and, thus, C(H) atoms have a smaller positive charge than C(F) atoms. On the contrary, the π atomic populations of the carbon atoms increase with the number of fluorine atoms. Thus, it can be concluded that the fluorine substituents act as π electron donors. However, the largest changes occur in the σ components, clearly showing that the fluorine σ electron withdrawing effect is dominant by far. The gross atomic populations of both the hydrogen and fluorine atoms do not change appreciably with substitution. In the case of the hydrogen atoms, this may be easily correlated with the fact that, as hydrogen does not have π orbitals easily accessible to make bonds, these atoms are not susceptible of changes in the hybridization state [41]. In turn, the fact that the gross atomic populations of the fluorine atoms (and their σ and π components) do not change appreciably with substitution indicates that, in the ions, both the σ electron withdrawing and π electron releasing ability of a fluorine atom are not affected significantly by its chemical environment.

Table 10 shows the Mulliken net atomic populations and the overlap populations calculated for the studied ions. The net atomic populations of the carbon atoms increase with the number of fluorine atoms, i.e. they show the opposite behavior to that followed by the corresponding gross atomic populations. In fact, this apparent discrepancy results from the considerable reduction of the C–C overlap populations with the number of fluorine atoms (for instance, χ_0C(H)–C(H) reduces by about 0.120 e, χ_0C(F)–C(H) by about 0.080 e, and χ_0C(F)–C(F) by above 0.050 e). Thus, H → F substitutions lead to an electron charge transfer from the C–C bonds to the carbon atoms. Indeed, this result agrees with the general increase found in the C–C bond lengths — either C(H)–C(H), C(F)–C(H) or C(F)–C(F) — with H → F substitutions (see Table 8), and may be easily understood, considering that progressive substitutions lead to increases in the electronegativity of the carbon atoms. The net atomic populations of the hydrogen atoms decrease slightly with substitution, while the C–H overlap populations do not vary. Hence, the calculated changes in the net atomic populations of hydrogen

Table 10
Mulliken net atomic populations (χ_n) and overlap population (χ_O) of **CP**, **MFCP**, **DFCP** and **TFCP**, calculated with the 6-311+G* basis set[a]

Molecule	χ_n(C(H))	π_n(C(H))	σ_n(C(H))	χ_n(C(F))	π_n(C(F))	σ_n(C(F))	χ_n(F)	π_n(F)	σ_n(F)	χ_n(H)			
CP	4.783	0.301	4.481							0.293			
MFCP	4.863	0.220	4.643	4.674	0.238	4.437	9.029	0.919	8.110	0.279			
DFCP	4.894	0.342	4.553	4.823	0.360	4.463	9.034	1.357	7.668	0.270			
TFCP				4.934	0.267	4.668	9.039	0.922	8.118				
	χ_O (C(H)–C(H))	π_O (C(H)–C(H))	σ_O (C(H)–C(H))	χ_O (C(H)–C(F))	π_O (C(F)–C(H))	σ_O (C(F)–C(H))	χ_O (C(F)–C(F))	π_O (C(F)–C(F))	σ_O (C(F)–C(F))	χ_O (C–F)	π_O (C–F)	σ_O (C–F)	χ_O (C–H)
CP	0.454	0.132	0.323										0.310
MFCP	0.332	0.135	0.196	0.450	0.149	0.301				0.215	0.059	0.156	0.315
DFCP				0.363	0.138	0.225	0.307	0.130	0.177	0.192	0.059	0.133	0.315
TFCP							0.253	0.136	0.117	0.169	0.056	0.113	

[a] In units of e ($e = 1.60219 \times 10^{-19}$ C).

are similar to those found in the gross atomic populations. Finally, both the net atomic populations of the fluorine atom and the C–F overlap populations do not change appreciably with the number of $H \rightarrow F$ substitutions, thus reinforcing our previous conclusion that, in these ions the electronic effects due to a fluorine atom are essentially equal and independent of the number of fluorine substituents.

From the analysis of the π/σ partitioning of the net atomic populations and of the overlap populations, also shown in Table 10, the following conclusions can be drawn:

(i) The π C–C (either C(H)–C(H), C(F)–C(H), or C(F)–C(F)) overlap populations do not change appreciably with the $H \rightarrow F$ substitutions. In addition, they do not correlate with the C–C bond lengths. This result is particularly interesting, as it shows that mesomerism does not play an important role in determining the relative values of the C–C bond lengths in the series of ions studied. Consequently, an explanation of the geometries of **MFCP** and **DFCP** in terms of dominant contributions of the resonance structures shown below is not supported by the results.

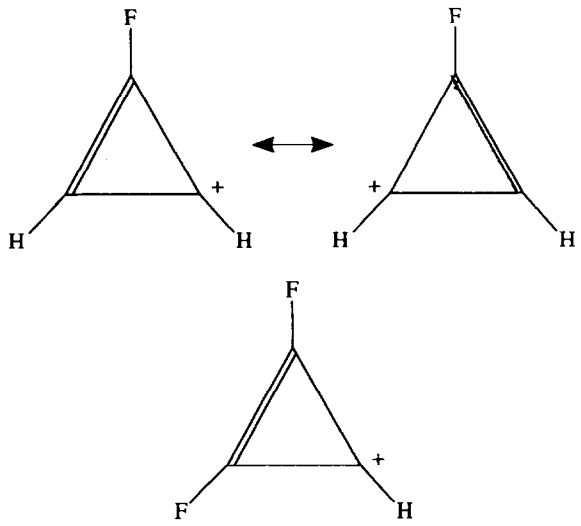

Indeed, it is the σ system (in particular the σ system re-hybridization processes explained above) that determines the relative values of the C–C bond lengths in the studied ions. A good relationship was found between the increase in the σ C–C overlap populations and the decrease of the C–C bond lengths (Fig. 4).

(ii) Both the π and σ net atomic populations present a complex and non-systematic pattern of variation with the increase in the number of $H \rightarrow F$ substitutions. This complex behavior may be due, at least in part, to processes of electron charge transferring involving the fluorine lone electron pairs, though re-hybridization itself may also play an important role in this finding.

In summary, a detailed analysis of the calculated (6-311+G*) electron distribution of the ions, in particular the changes in the electron distribution associated with successive $H \rightarrow F$ substitutions, leads to the conclusion that re-hybridization induced in the carbon atoms by the fluorine substituents and the fluorine σ electron withdrawing ability are the main factors which determine their electronic properties. In addition, the differences found in the geometrical parameters of the ions may also be explained, in electronic terms, by considering these two factors. On the contrary, the π system was found to be little affected by the $H \rightarrow F$ substitutions and does not play any relevant role in determining the relative values of the C–C bond lengths in the studied ions. Finally, each fluorine substituent was found to act almost independently of the others.

3.3. Vibrational analysis

Table 11 shows the symmetry coordinates used in this study to perform the vibrational calculations. Four isotopomers of **CP** were considered ($C_3H_3^+$, $C_3H_2D^+$, $C_3D_2H^+$ and $C_3D_3^+$), three of **MFCP** ($C_3H_2F^+$, C_3HDF^+ and $C_3D_2F^+$), two of **DFCP** ($C_3HF_2^+$ and $C_3DF_2^+$) and one of **TFCP** ($C_3F_3^+$). The results are summarized in Tables 12–15, where the 6-311+G* calculated (scaled) frequencies are compared with the experimental values. The fitting of the calculated to the experimental frequencies (scaling) yields the straight line shown in Fig. 5. The general agreement between the calculated and the experimental values is remarkably good for all types of normal modes (with a few exceptions, the agreement of the experimental and calculated frequencies is within

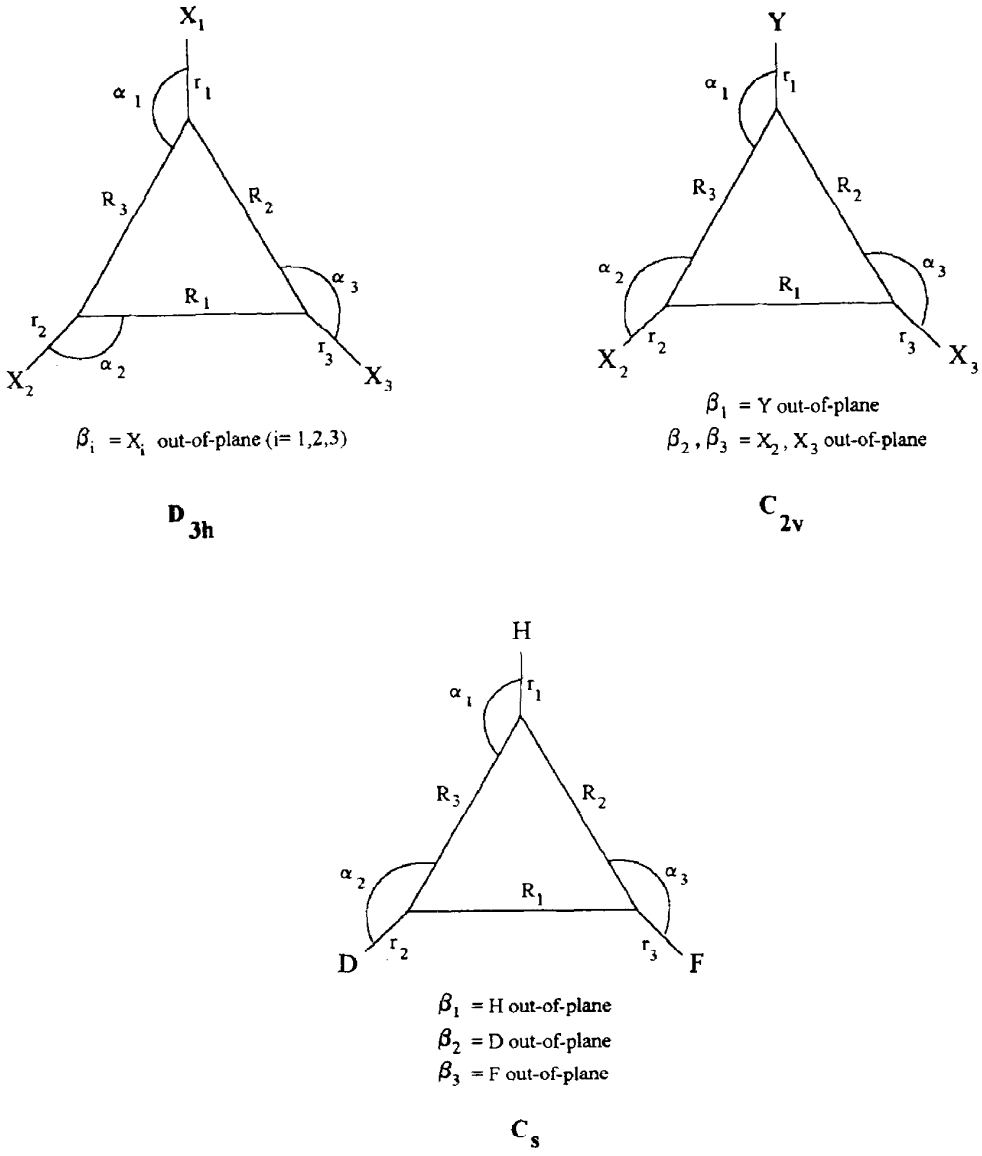

Fig. 3. Internal coordinates definition. X, Y = H, D, F.

2%, and the largest error — which occurs for a very low frequency mode of **TFCP** — amounts to about 5%, corresponding to only a $16\,cm^{-1}$ absolute deviation). This excellent general agreement is noteworthy and constitutes additional evidence of the good quality of the electron distribution obtained using the 6-311+G* basis set.

In the case of the **CP** and its deuterated isotopomers, the present calculations give further support to the assignments previously made [15]. For the fluorosubstituted cations, they enable us to confirm or reassign some of the observed bands [21–23]. The new assignments are discussed below:

$C_3H_2F^+$. The bands at 1372 and $1339\,cm^{-1}$, previously ascribed doubtfully to the νC–C asym b_1 and νC–C a_1 vibrations, respectively [21], are now assigned inversely, as the calculations clearly

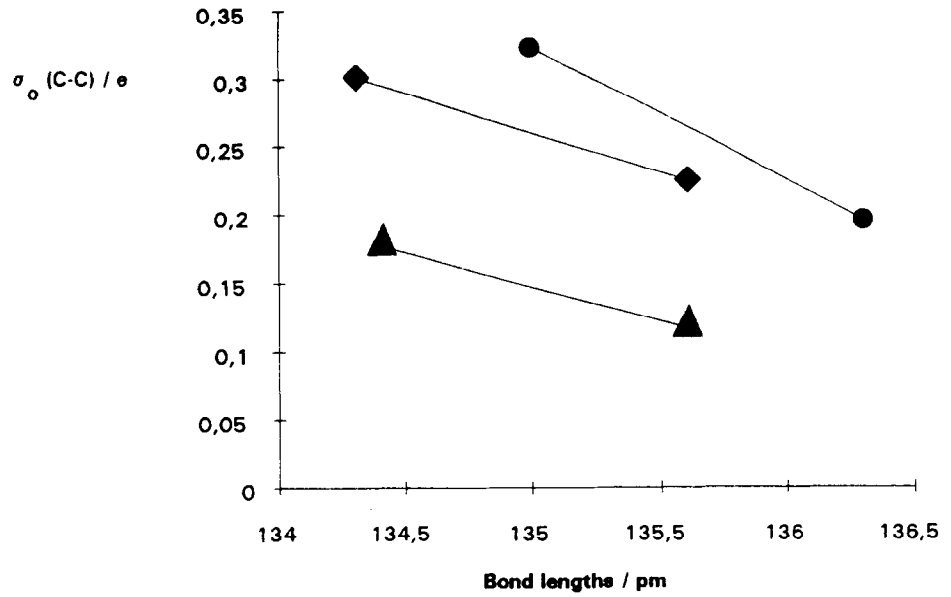

Fig. 4. 6-311+G* calculated σ_0 (C–C) overlap populations vs. C–C bond lengths: ● C(H)–C(H); ◆ C(H)–C(F); ▲ C(F)–C(F).

predict that the a_1 mode has a higher frequency than the b_1 vibration. The same happens with respect to the ωCF b_2 and δCF b_1 normal modes, which are now also reassigned inversely to the tentative assignments made in Ref. [21]. Thus, the b_2 mode is now assigned to the band at 483 cm^{-1} (calculated frequency 485 cm^{-1}), while the b_1 mode is ascribed to the shoulder appearing at 477 cm^{-1} (calculated value, 476 cm^{-1}). The unobserved ωCH asym a_2 vibration is predicted to have a frequency very close to that of the δCH sym a_1 mode (996 vs. 993 cm^{-1}) and is probably hidden underneath the band ascribed to this latter vibration (about 990 cm^{-1}). The previously suggested frequency for the ωCH asym a_2 mode (944 cm^{-1}, based in a simplified valence force field normal coordinate analysis [21]) is thus considerably underestimated. This conclusion is further reinforced by looking at both the experimental and calculated frequencies for this vibration in $C_3H_2D^+$ (997 and 990 cm^{-1}, respectively, see Table 12).

$C_3D_2F^+$. As in the case of the non-deuterated fluorocyclopropenyl cation, the bands previously ascribed to the νC–C asym b_1 and νC–C a_1 vibrations are now assigned inversely. In turn, the band at 828 cm^{-1}, previously assigned to the δCD asym b_1 mode [21], is now reassigned to the ωCD asym a_2 vibration (calculated value 813 cm^{-1}). No assignment for the a_2 mode was given in Ref. [21], while it was wrongly predicted to occur at about 765 cm^{-1} (value calculated from normal coordinate analysis using a simplified valence force field). To the δCD asymb b_1 mode (calculated value 842 cm^{-1}) is now assigned the band at 875 cm^{-1} appearing in the IR spectrum of the $Sb_2F_{11}^-$ salt of the $C_3D_2F^+$ cation that was not ascribed previously [21].

$C_3HF_2^+$. All previous assingments [22] of this cation and its deuterated analogue, $C_3DF_2^+$, are confirmed by the present calculations. In addition, it is now shown that the band at 924 cm^{-1} in the spectra of the non-deuterated molecule corresponds to the νC–F asym b_1 mode (calculated value 935 cm^{-1}). In Ref. [22], this band was assigned doubtfully to either this mode or the ωCH b_1 vibration. However, this latter has a slightly larger frequency (calculated value 942 cm^{-1}) and should correspond to the band observed at 946 cm^{-1} or, at least, contribute to it (in the experimental study, this band was assigned to a vibration of the fluorosulfite ester cation $C_3FHSO_2F^+$, which is formed from $C_3HF_2^+$ and the solvent (SO_2) when the temperature is raised above −25°C). The ωCH b_1 vibration in $C_3HD_2^+$

Table 11
Definition of symmetry coordinates[a]

Symmetry species	Coordinate	Approximate description	Definition
$C_3X_3^+$ (Point group: D_{3h})			
a_1'	S_1	νC–X sym	$(\Delta r_1 + \Delta r_2 + \Delta r_3)/\sqrt{3}$
a_1'	S_2	νC–C sym	$(\Delta R_1 + \Delta R_2 + \Delta R_3)/\sqrt{3}$
a_2'	S_3	δCX sym	$(\Delta\alpha_1 + \Delta\alpha_2 + \Delta\alpha_3)/\sqrt{3}$
e'	S_{4a}	νC–X asym (a)	$(2\Delta r_1 - \Delta r_2 - \Delta r_3)/2$
e'	S_{4b}	νC–X asym (b)	$(\Delta r_2 - \Delta r_3)/\sqrt{2}$
e'	S_{5a}	νC–C asym (a)	$(2\Delta R_1 - \Delta R_2 - \Delta R_3)/2$
e'	S_{5b}	νC–C asym (b)	$(\Delta R_2 - \Delta R_3)/\sqrt{2}$
e'	S_{6a}	δCX asym	$(2\Delta\alpha_1 - \Delta\alpha_2 - \Delta\alpha_3)/2$
e'	S_{6b}	δCX asym	$(\Delta\alpha_2 - \Delta\alpha_3)/\sqrt{2}$
a_2''	S_7	ωCX sym	$(\Delta\beta_1 + \Delta\beta_2 + \Delta\beta_3)\sqrt{3}$
e''	S_{8a}	ωCX asym (a)	$(2\Delta\beta_1 - \Delta\beta_2 - \Delta\beta_3)/2$
e''	S_{8b}	ωCX asym (b)	$(\Delta\beta_2 + \Delta\beta_3)\sqrt{2}$
$C_3X_2Y^+$ (Point group: C_{2v})			
a_1	S_1	νC–X sym	$(\Delta r_2 + \Delta r_3)/\sqrt{2}$
a_1	S_2	νC–Y	Δr_1
a_1	S_3	νC–C sym	$(\Delta R_2 + \Delta R_3)/\sqrt{2}$
a_1	S_4	νC–C	ΔR_1
a_1	S_5	δCX sym	$(\Delta\alpha_2 + \Delta\alpha_3)/\sqrt{2}$
a_2	S_6	ωCX asym	$(\Delta\beta_2 - \Delta\beta_3)/\sqrt{2}$
b_1	S_7	νC–X asym	$(\Delta r_2 - \Delta r_3)/\sqrt{2}$
b_1	S_8	νC–C asym	$(\Delta R_2 - \Delta R_3)/\sqrt{2}$
b_1	S_9	δCX asym	$(\Delta\alpha_2 - \Delta\alpha_3)/\sqrt{2}$
b_1	S_{10}	δCY	$\Delta\alpha_1$
b_2	S_{11}	ωCX sym	$(\Delta\beta_2 + \Delta\beta_3)/\sqrt{2}$
b_2	S_{12}	ωCY	$\Delta\beta_1$
C_3HDF^+ (Point group: C_S)			
a'	S_1	νC–H	Δr_1
a'	S_2	νC–D	Δr_2
a'	S_3	νC–F	Δr_3
a'	S_4	νC–C (1)	ΔR_1
a'	S_5	νC–C (2)	ΔR_2
a'	S_6	νC–C (3)	ΔR_3
a'	S_7	δCH	$\Delta\alpha_1$
a'	S_8	δCD	$\Delta\alpha_2$
a'	S_9	δCF	$\Delta\alpha_3$
a''	S_{10}	ωCH	$\Delta\beta_1$
a''	S_{11}	ωCD	$\Delta\beta_2$
a''	S_{12}	ωCF	$\Delta\beta_3$

[a] X, Y = H, D, F; see Fig. 3 for definition of the internal coordinates; ν, stretching; δ, in-plane bending, ω, out-of-plane bending; sym, symmetric; asym, asymmetric.

gives rise to a band at about 960 cm^{-1} (see Table 12) which reinforces the present assignments.

$C_3F_3^+$. The calculations confirm the assignments previously made [23]. However, two modes remained to be assigned in the experimental work (δCF sym a_2' and ωCF sym a_2''). These were predicted to give rise to frequencies at about 811 and 239 cm^{-1}, respectively, by normal coordinate analysis using a simplified valence force field [23]. However, the present calculations show that these values were considerably overestimated and underestimated, respectively. In fact, the 6-311+G*

Table 12
Calculated and experimental vibrational frequencies (cm^{-1}) of $C_3H_3^+$, $C_3H_2D^+$, $C_3D_2H^+$ and $C_3D_3^+$ and corresponding potential energy distribution (PED)[a]

Approximate description	Symmetry	Exp.[b]	Calc.	PED[c]
$C_3H_3^+$				
νC–H sym	a_1'	3183	3186	$S_1[95] + S_2[5]$
νC–H asym	e'	3138	3136	$S_4(a)[64] + S_4(b)[35]$
νC–C sym	a_1'	1626	1619	$S_2[96] + S_1[5]$
νC–C asym	e'	1290	1276	$S_5(a)[49] + S_5(b)[45] + S_6(a)[17]$
δCH sym	a_2'	1031[d]	1047	$S_3[100]$
ωCH asym	e''	990[d]	998	$S_8(a)[98]$
δCH asym	e'	927	925	$S_6(a)[83] + S_5(b)[10]$
ωCH sym	a_2''	758	761	$S_7[100]$
$C_3H_2D^+$				
νC–H sym	a_1	3166[e]	3169	$S_1[96]$
νC–H asym	b_1	3134	3136	$S_7[99]$
νC–D	a_1	2389	2373	$S_2[89] + S_3[11]$
νC–C sym	a_1	1583	1572	$S_3[52] + S_4[45] + S_2[8]$
νC–C asym	b_1	1286	1270	$S_8[95] + S_{10}[6]$
νC–C	a_1	1267	1253	$S_4[50] + S_3[34] + S_5[28]$
δCH asym	b_1	1008[d]	1021	$S_9[97] + S_{10}[9]$
ωCH asym	a_2	990[d]	997	$S_6[100]$
δCH sym	a_1	924	923	$S_5[76] + S_4[7]$
ωCH sym	b_2	920	911	$S_{11}[68] + S_{12}[23]$
δCD	b_1	718	716	$S_{10}[87]$
ωCD	b_2	655[d]	656	$S_{12}[78] + S_{11}[33]$
$C_3D_2H^+$				
νC–H	a_1	3154	3154	$S_2[98]$
νC–D sym	a_1	2420	2418	$S_1[84] + S_4[10] + S_3[6]$
νC–D asym	b_1	2354	2326	$S_7[96]$
νC–C sym	a_1	1536[e]	1527	$S_3[71] + S_4[20] + S_1[14]$
νC–C	a_1	1268	1252	$S_4[72] + S_3[21] + S_5[17]$
νC–C asym	b_1	1256	1242	$S_8[88] + S_{10}[14]$
δCH	b_1	973	985	$S_{10}[80] + S_9[13] + S_8[6]$
ωCH	b_2	960	959	$S_{12}[86] + S_{11}[9]$
ωCD asym	a_2	807	809	$S_{11}[100]$
δCD sym	a_1	767	767	$S_9[89] + S_{10}[7]$
δCD asym	b_1	675	670	$S_5[87]$
ωCD sym	b_2	603	601	$S_{11}[93] + S_{12}[15]$
$C_3D_3^+$				
νC–D sym	a_1'	2471[e]	2461	$S_1[79] + S_2[20]$
νC–D asym	e'	2348	2326	$S_4(a)[58] + S_4(b)[38]$
νC–C sym	a_1'	1490	1481	$S_2[80] + S_1[20]$
νC–C asym	e'	1248	1232	$S_5(a)[62] + S_5(b)[34] + S_6(b)[13]$
δCD sym	a_2'	837[d]	849	$S_3[100]$
ωCD asym	e''	802	809	$S_8(a)[95] + S_8(b)[6]$
δCD asym	e'	674	668	$S_6(a)[89] + S_5(b)[6]$
ωCD sym	a_2''	*560*	557	$S_7[100]$

[a] See Table 11 for definition of symmetry coordinates; ν, stretching; δ, in-plane bending; ω; out-of-plane bending; sym, symmetric; asym, asymmetric.

[b] From spectra in SO_2 solution [15]. Value in italic was obtained from the $C_3D_3^+$ salt of BF_4^- [15].

[c] Only PEDs greater than 5% are shown; in the case of degenerate modes, only the PED corresponding to that vibration involving mainly the (*a*) coordinate is shown.

[d] Calculated values [15] including anharmonic corrections.

[e] Modified for excluding Fermi resonance [15].

Table 13
Calculated and experimental vibrational frequencies (cm^{-1}) of $C_3H_2F^+$, C_3HDF^+ and $C_3D_2F^+$ and corresponding potential energy distribution (PED)[a]

Approximate description	Symmetry	Exp.[b]	Cal.	PED[c]
$C_3H_2F^+$				
νC–H sym	a_1	3153	3159	$S_1[96]$
νC–H asym	b_1	3119	3130	$S_7[99]$
νC–C sym	a_1	1835	1858	$S_3[63] + S_2[39] + S_4[7]$
νC–C	a_1	1372	1365	$S_4[85] + S_2[17] + S_5[14]$
νC–C asym	b_1	1339	1340	$S_8[91] + S_{10}[6]$
δCH asym	b_1	*1022*	1033	$S_9[99] + S_{10}[8]$
ωCH asym	a_2	n.o.	996	$S_6[100]$
δCH sym	a_1	988	993	$S_5[73] + S_2[22] + S_3[13]$
ωCH sym	b_2	*876*	883	$S_{11}[83] + S_{12}[11]$
νC–F	a_1	830	832	$S_3[27] + S_2[23] + S_5[18] + S_4[12]$
ωCF	b_2	483	485	$S_{12}[91] + S_{11}[20]$
δCF	b_1	477	476	$S_{10}[87] + S_8[7]$
C_3HDF^+				
νCH	a'	–	3144	$S_1[98]$
νC–D	a'	–	2374	$S_2[87] + S_4[8] + S_6[5]$
νC–C (2)	a'	–	1836	$S_3[49] + S_5[36] + S_4[26] + S_2[7]$
νC–C (3)	a'	–	1349	$S_6[61] + S_5[14] + S_4[13] + S_3[12]$
νC–C (1)	a'	–	1305	$S_4[31] + S_5[28] + S_6[24] + S_9[8] + S_2[5]$
δCH	a'	–	1011	$S_7[88] + S_3[8] + S_4[5]$
ωCH	a''	–	952	$S_{10}[87] + S_{11}[6]$
νC–F	a'	–	904	$S_3[33] + S_8[30] + S_5[17] + S_4[14] + S_9[7]$
ωCD	a''	–	761	$S_{11}[72] + S_{12}[20]$
δCD	a'	–	718	$S_8[58] + S_6[6] + S_7[5]$
ωCF	a''	–	457	$S_{12}[80] + S_{11}[24] + S_{10}[12]$
δCF	a'	–	452	$S_9[80] + S_8[9]$
$C_3D_2F^+$				
νC–D sym	a_1	2426	2419	$S_1[81] + S_4[10] + S_3[10]$
νC–D asym	b_1	2353	2327	$S_7[95] + S_8[5]$
νC–C sym	a_1	1790	1802	$S_3[54] + S_2[44] + S_1[11]$
νC–C	a_1	*1331*	1306	$S_4[86] + S_2[12] + S_5[10] + S_1[7]$
νC–C asym	b_1	1289	1296	$S_8[89] + S_{10}[7]$
νC–F	a_1	914	914	$S_2[42] + S_3[35] + S_5[22]$
δCD asym	b_1	*875*	842	$S_7[90] + S_{10}[17]$
ωCD asym	a_2	828	813	$S_6[100]$
ωCD sym	b_2	*732*	742	$S_{11}[60] + S_{12}[30]$
δCD sym	a_1	650	645	$S_5[73] + S_4[6] + S_3[5]$
δCF	b_1	446	435	$S_{10}[77] + S_7[12] + S_8[8]$
ωCF	b_2	424	428	$S_{12}[72] + S_{11}[43]$

[a] See Table 11 for definition of symmetry coordinates; ν, stretching; δ, in-plane bending; ω, out-of-plane bending; sym, symmetric; asym, asymmetric; n.o., not observed.
[b] From spectra in SO_2 solution [21]; values in italic were obtained for $C_3H_2F^+$ or $C_3D_2F^+$ salts of BF_4^- or $Sb_2F_{11}^-$ [21].
[c] Only PEDs greater than 5% are shown.

(scaled) calculated frequency for the δCF sym a_2' mode is 769 cm^{-1}, while that corresponding to the ωCF sym a_2'' vibrations is 256 cm^{-1}. It is interesting to note that bands close to these two frequencies were observed experimentally (767 and 257 cm^{-1} [23]), though they were assigned in the experimental work to other species (BF_4^- and $C_3F_4/B_2F_7^-$ or $Sb_2F_{11}^-$). Indeed, we believe that the two vibrations of the $C_3F_3^+$ cation not assigned previously contribute in some extent to these bands.

Table 14
Calculated and experimental vibrational frequencies (cm^{-1}) of $C_3HF_2^+$ and $C_3DF_2^+$ and corresponding potential energy distribution (PED)[a]

Approximate description	Symmetry	Exp.[b]	Calc.	PED[c]
$C_3HF_2^+$				
νC–H	a_1	3126	3136	$S_2[98]$
νC–C	a_1	1945	1969	$S_1[43] + S_4[40] + S_3[30]$
νC–C asym	b_1	*1541*	1582	$S_7[67] + S_8[46]$
νC–C sym	a_1	1393	1383	$S_3[59] + S_4[25] + S_5[16]$
δCH	b_1	*1025*	1058	$S_{10}[72] + S_7[16] + S_8[14]$
ωCH	b_2	946	942	$S_{12}[90]$
νC–F asym	b_1	924	935	$S_8[34] + S_{10}[21] + S_7[18] + S_9[13]$
νCF sym	a_1	843	844	$S_1[53] + S_4[31] + S_3[8] + S_5[7]$
ωCF asym	a_2	650	664	$S_6[100]$
δCF asym	b_1	582	584	$S_9[89] + S_8[11] + S_{10}[5]$
ωCF sym	b_2	366	364	$S_{11}[100] + S_{12}[13]$
δCF sym	a_1	311	296	$S_5[79] + S_4[8]$
$C_3DF_2^+$				
νC–D	a_1	2379	2375	$S_2[84] + S_3[14]$
νC–C	a_1	1923	1938	$S_1[44] + S_4[42] + S_3[19] + S_2[8]$
νC–C asym	b_1	*1540*	1580	$S_7[67] + S_8[46]$
νC–C sym	a_1	1347	1333	$S_3[57] + S_4[23] + S_5[16] + S_2[7]$
νC–F asym	b_1	971	988	$S_8[46] + S_7[33] + S_{10}[13]$
νC–F sym	a_1	837	839	$S_1[53] + S_4[30] + S_3[10] + S_5[6]$
δCD	b_1	806	823	$S_{10}[61] + S_9[40]$
ωCD	b_2	*762*	774	$S_{12}[81] + S_{11}[10]$
ωCF asym	a_2	650	664	$S_6[100]$
δCF asym	b_1	*521*	513	$S_9[64] + S_{10}[25] + S_8[11]$
ωCF sym	b_2	340	337	$S_{11}[94] + S_{12}[22]$
δCF sym	a_1	309	294	$S_5[79] + S4[8]$

[a] See Table 11 for definition of symmetry coordinates; ν, stretching; δ, in-plane bending; ω, out-of-plane bending; sym, symmetric; asym, asymmetric.
[b] From spectra in SO_2 solution [22]; values in italic were obtained for $C_3HF_2^+$ or $C_3DF_2^+$ salts of BF_4^- or $Sb_2F_{11}^-$ [22].
[c] Only PEDs greater than 5% are shown.

Table 15
Calculated and experimental vibrational frequencies (cm^{-1}) of $C_3F_3^+$ and corresponding potential energy distribution (PED)[a]

Approximate description	Symmetry	Exp.[b]	Calc.	PED[c]
$C_3F_3^+$				
νC–C sym	a_1'	2014	2045	$S_2[62] + S_1[45]$
νC–C asym	e'	*1590*	1612	$S_4(a)[48] + S_5(a)[38] + S_4(b)[15] + S_5(b)[12] + S_6(a)[5]$
νC–F asym	e'	999	1006	$S_5(a)[25] + S_4(a)[22] + S_5(b)[18] + S_4(b)[16] + S_6(b)[13]$
δCF sym	a_2'	767	769	$S_3[100]$
νC–F sym	a_1'	752	752	$S_1[55] + S_2[38]$
ωCF asym	e''	642	660	$S_8(a)[100]$
δCF asym	e'	287	271	$S_6(a)[85] + S_5(b)[14]$
ωCF sym	a_2''	257	256	$S_7[100]$

[a] See Table 11 for definition of symmetry coordinates; ν, stretching; δ, in-plane bending; ω, out-of-plane bending; sym, symmetric; asym, asymmetric.
[b] From spectra in SO_2 solution [23]; value in italic was obtained for the $C_3F_3^+$ salt of BF_4^- [23].
[c] Only PEDs greater than 5% are shown; in the case of degenerate modes, only the PED corresponding to that vibration involving mainly the (*a*) coordinate is shown.

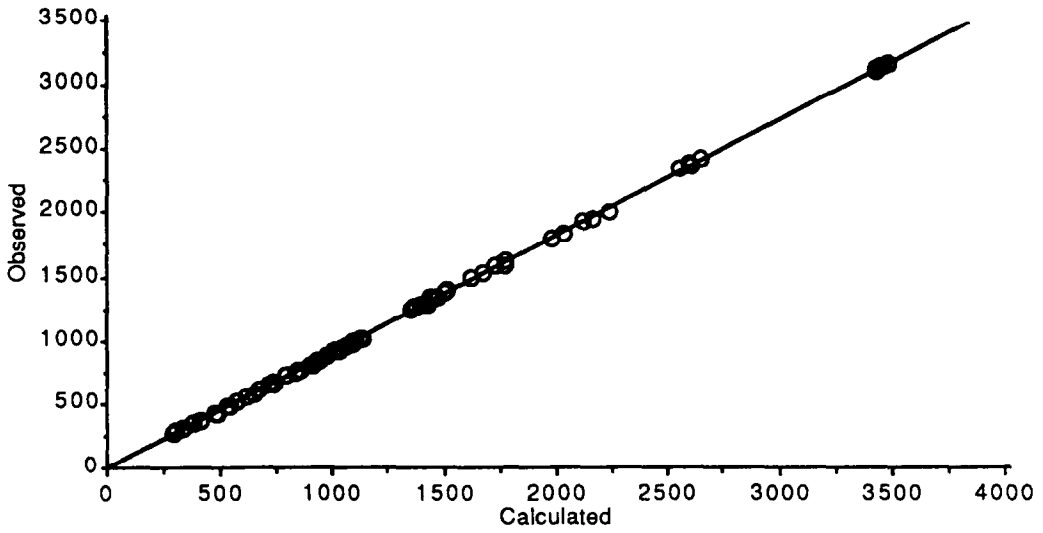

Fig. 5. Calculated vs. experimental vibrational frequencies (cm^{-1}) for **CP**, **MFCP**, **DFCP** and **TFCP**. The straight line resulting from the linear regression is $\nu_{Obs.} = 0.916 \times \nu_{Cal.} - 8.329$; $R^2 = 1$.

The analysis of the potential energy distributions (PEDs) for the various molecules studied here (see Tables 12–15) leads essentially to the same conclusions previously reported in Refs. [15] and [21–23]. The following trends can be drawn:

(i) For the cyclopropenyl cation (and its isotopomers), as well as for the monofluorosubstituted molecules, most of the normal modes are dominated by a single symmetry coordinate.

(ii) In the deuterated compounds some mixing of coordinates can be noticed involving the symmetric C–C and C–D stretching coordinates.

(iii) Increasing the number of hydrogen-by-fluorine substitutions increases the degree of mixing of the symmetry coordinates. In the monofluorosubstituted cation, the C–F stretching mixes mainly with the C–C symmetric stretching associated with the two adjacent C–C bonds (see Table 13); in the disubstituted cation, both the symmetric and the antisymmetric C–F stretching coordinates mix strongly with the C C stretching coordinates (the first, with the two C–C stretching coordinates of a_1 symmetry and the second with the C–C antisymmetric stretching coordinate; see Table 14); finally, in the trisubstituted cation, again the C–F symmetric and antisymmetric stretching oscillators mix considerably with the C–C symmetric and antisymmetric stretching coordinates, respectively.

(iv) The extensive mixing observed between the C–C and C–F stretching coordinates leads to notably high frequencies for the ring breathing mode in **TFCP** as well as for the ring mode involving mainly the C(F)–C bonds or the C(F)–C(F) bond in **MFCP** or **DFCP**, respectively.

Acknowledgments

The authors are grateful to Professors Mozart N. Ramos (Departamento de Química Fundamental, Universidade Federal de Pernambuco, Brazil) and Hugh D. Burrows (Departamento de Química, Universidade de Coimbra, Portugal) for their helpful comments and suggestions, and to Gustavo L.C. Moura and Huang S. Ciz for their aid in preliminary calculations. This research was financially supported by Junta Nacional de Investigação Científica e Tecnológica (JNICT), Portugal, and Conselho Nacional de Pesquisas (CNP_q), Brazil.

References

[1] R.D. Kern, H.J. Singh and K. Xie, J. Phys. Chem., 94 (1990) 3333.

[2] J.M. Goodings, D.K. Bohme and C.-W. Ng, Combust. Flame, 36 (1979) 27.
[3] D.B. Olson and H.F. Calcote, Proc. 18th Int. Symp. on Combusion, 1981, p. 453.
[4] P. Michauld, J.L. Delfau and A. Barrasin, Proc. 18th Int. Symp. on Combustion, 1981, p. 443.
[5] S.A. Korth, M.L. Marconi, D.A. Mendis, F.A. Krueger, A.K. Richter, R.P. Lin, D.L. Mitchell, K.A. Anderson, C.W. Carlson, H. Rème, J.A. Sauvaud and C. d'Uston, Nature, 337 (1989) 52.
[6] F.P. Losing, Can. J. Chem., 50 (1972) 3971.
[7] P.J. Ausloos and S.G. Lias, J. Am. Chem. Soc., 103 (1981) 6505.
[8] A. Cameron, J. Leszczynky, M.C. Zerner and B. Weiner, J. Phys. Chem., 93 (1989) 139.
[9] L. Radom, P.C. Hariharan, J.A. Pople and P.v.R. Schleyer, J. Am. Chem. Soc., 98 (1976) 10.
[10] K. Raghavachari, R.A. Whiteside, J.A. Pople and P.v.R. Schleyer, J. Am. Chem. Soc., 103 (1981) 5649.
[11] M.W. Wang and L. Radom, J. Am. Chem. Soc., 111 (1989) 6976.
[12] A.C. Hopkinson and M.H. Lien, J. Am. Chem. Soc., 108 (1986) 2843.
[13] R. Breslow and J.T. Groves, J. Am. Chem. Soc., 92 (1970) 988.
[14] T. Takada and K. Ohno, Bull. Chem. Soc. Jpn., 52 (1979) 334.
[15] N. Craig, J. Pranata, S.J. Reiganum, J.R. Sprague and P.S. Stevens, J. Am. Chem. Soc., 108 (1986) 4378.
[16] T.K. Ha, F. Graf and H. Gunthard, J. Mol. Struct., 15 (1973) 335.
[17] Y.-G. Buyn, S. Saebo and C.U. Pittman, Jr., J. Am. Chem. Soc., 113 (1991) 3689.
[18] Y. Xie and J.E. Boggs, J. Chem. Phys., 90 (1989) 4320.
[19] T.J. Lee, A. Willets, G.F. Jeffrey and N.C. Handy, J. Chem. Phys., 90 (1989) 4330.
[20] T.D. Norden, S.W. Staley, W.H. Taylor and M.D. Harmony, J. Am. Chem. Soc., 108 (1986) 7912.
[21] N.C. Craig, R.K.-Y. Lai, L.G. Matus, J.H. Miller and S.L. Palfrey, J. Am. Chem. Soc., 102 (1980) 36.
[22] N.C. Craig, R.K.-Y. Lai, K.W. Penfield and I.W. Levin, J. Phys. Chem., 84 (1980) 899.
[23] N.C. Craig, N.C. Fleming and J. Pranata, J. Am. Chem. Soc., 107 (1985) 7324.
[24] M.H. Lien and A.C. Hopkinson, J. Mol. Struct. (Theochem) 165 (1988) 37.
[25] T. Clark, J. Chandrasekar, G.W. Spitznagel and P.v.R. Schleyer, J. Comput. Chem., 4 (1983) 294.
[26] M.J. Frisch, M. Head-Gordon, G.W. Trucks, J.B. Foresman, H.B. Schlegel, K. Raghavachari, M. Robb, M. Binkley, C. Gonzalez, D.J. Defrees, D.J. Fox, R.A. Whiteside, R. Seegler, C.F. Melius, J. Baker, R.L. Martin, L.R. Kahn, J.J.P. Stewart, S. Topiol and J.A. Pople, GAUSIAN 90, revision F, Gaussian, Inc., Pittsburgh PA, 1990.
[27] R. Krishnan, J.S. Binkely, R. Seeger and J.A. Pople, J. Chem. Phys., 72 (1980) 4244.
[28] M.D.G. Faria and R. Fausto, TRANSFORMER (version 1.0), Departamento de Química, Universidade de Coimbra, Portugal, 1990.
[29] M.D.G. Faria and R. Fausto, BUILD-G and VIBRAT, Departamento de Química, Universidade de Coimbra, Portugal, 1990 (These programs incorporate several routines from programs GMAT and FPERT, H Fuher, V.B Kartha, K.G. Kidd, P.J. Krueger and H.H. Mantsch, Natl. Res. Counc. Can. Bull., 15 (1976) 1).
[30] R.S. Grev and H.F. Schaefer, J. Chem. Phys., 91 (1989) 7305.
[31] D.B. Chesnut and K.D. Moore, J. Chem. Phys., 96 (1992) 7188.
[32] M. Gussoni, M.N. Ramos, C. Castiglioni and G. Zerbi, Chem. Phys. Lett., 142 (1987) 515.
[33] W.T. King and G.B. Mast, J. Phys. Chem., 80 (1980) 2521.
[34] U. Dinur, Chem. Phys. Lett., 166 (1990) 211.
[35] M.H. Lien and A.C. Hopkinson, J. Mol Struct. (Theochem), 121 (1985) 1.
[36] A.T. Peretta and V.W. Laurie, J. Chem. Phys., 62 (1975) 246.
[37] K.R. Ramaprasad, V.W. Laurie and N.C. Craig, J. Chem. Phys., 64 (1977) 3896.
[38] L. Pierce and V. Dobyns, J. Am. Chem. Soc., 84 (1962) 2651.
[39] J.L. Hencher and S.H. Bauer, J. Am. Chem. Soc., 89 (1967) 5527.
[40] K.B. Wiberg and K.E. Laidig, J. Am. Chem. Soc., 109 (1987) 5935.
[41] H.A. Bent, Chem. Rev., 61 (1961) 275.